

The far-ultraviolet spectra of “cool” PG 1159 stars

K. Werner¹, T. Rauch¹, and J. W. Kruk²

¹ Institute for Astronomy and Astrophysics, Kepler Center for Astro and Particle Physics, Eberhard Karls University, Sand 1, 72076 Tübingen, Germany
e-mail: werner@astro.uni-tuebingen.de

² NASA Goddard Space Flight Center, Greenbelt, MD 20771, USA

Received xx xx 2015 / Accepted xx xx 2015

ABSTRACT

We present a comprehensive study of Far Ultraviolet Spectroscopic Explorer (FUSE) spectra (912–1190 Å) of two members of the PG 1159 spectral class, which consists of hydrogen-deficient (pre-) white dwarfs with effective temperatures in the range $T_{\text{eff}} = 75\,000\text{--}200\,000$ K. As two representatives of the cooler objects, we have selected PG 1707+427 ($T_{\text{eff}} = 85\,000$ K) and PG 1424+535 ($T_{\text{eff}} = 110\,000$ K), complementing a previous study of the hotter prototype PG 1159–035 ($T_{\text{eff}} = 140\,000$ K). The helium-dominated atmospheres are strongly enriched in carbon and oxygen, therefore, their spectra are dominated by lines from C III–IV and O III–VI, many of which were never observed before in hot stars. In addition, lines of many other metals (N, F, Ne, Si, P, S, Ar, Fe) are detectable, demonstrating that observations in this spectral region are most rewarding when compared to the near-ultraviolet and optical wavelength bands. We perform abundance analyses of these species and derive upper limits for several undetected light and heavy metals including iron-group and trans-iron elements. The results are compared to predictions of stellar evolution models for neutron-capture nucleosynthesis and good agreement is found.

Key words. stars: abundances – stars: atmospheres – stars: evolution – stars: AGB and post-AGB – white dwarfs

1. Introduction

The overarching interest in PG 1159 stars is related to the investigation of nucleosynthesis processes in evolved low- to intermediate-mass stars during their asymptotic giant branch (AGB) stage. It is believed that these very hot, hydrogen-deficient (pre-) white dwarfs (WDs) exhibit their helium-dominated layer as a consequence of a late helium-shell flash (e.g., Werner & Herwig 2006). While usually kept hidden below the hydrogen-rich envelope, these stars allow us to investigate directly the chemistry of the H-He intershell region of the former red giant star in which neutron-capture nucleosynthesis shapes the metal abundance pattern. Spectroscopically, the access to metals heavier than C, N, and O requires far-ultraviolet observations shortward of about 1150 Å because the atoms are highly ionized. The search for weak metal lines is particularly difficult for the PG 1159 stars at the “cool” end (effective temperature $T_{\text{eff}} \approx 75\,000\text{--}120\,000$ K) of the T_{eff} range they cover (up to 200 000 K). This is because, as we demonstrate in this paper, a very large number of spectral lines from the CNO elements in ionization stages C III, N IV, O IV–V, appear in this lower temperature interval while hotter objects, like the prototype PG 1159–035 (140 000 K, Jahn et al. 2007) exhibit spectra with much fewer lines of the CNO elements appearing in higher ionization stages (C IV, N V, and O VI). Often, heavier metals can only be detected by a handful of lines at best, therefore, a good knowledge of potential line blends is important.

Here we investigate two relatively cool PG 1159 stars for which FUSE (Far Ultraviolet Spectroscopic Explorer) spectra are available. We have two aims. First we aim to compute model spectra to identify as many lines from the CNO elements as possible. This is initially interesting in itself because the relatively high abundance of these elements allows the detection of many

lines that are usually not seen in stellar spectra. In addition, it poses a challenge because it requires exceptionally large non-local thermodynamic equilibrium (non-LTE) model atoms with atomic data to be gathered from different sources. Second, based on these models we identify lines from heavier metals and perform abundance determinations, taking potential line blends into account.

Preliminary results of the related, substantial work to achieve these goals were published by our group in recent years as progress reports (Reiff et al. 2005, 2007, 2008; Müller-Ringat 2013). Based on this, we present here a comprehensive analysis with considerably extended model atoms and hitherto not studied species, leading to an unprecedented description and analysis of the far-ultraviolet (far-UV) spectra of cool PG 1159 stars. The paper is organized as follows. We introduce the two program stars in Sect. 2. Their FUSE spectra and our method of line identification are presented in Sect. 3. Model atmosphere calculations for the spectral analysis are specified in Sect. 4. Details of the line identification and results of our element abundance analysis are described in Sect. 5. A summary of the results and a discussion in the context of abundance predictions from stellar evolution theory in Sect. 6 conclude the paper.

2. The program stars

PG 1707+427 and PG 1424+535 were among the first stars classified as PG 1159 stars (Liebert & Stockman 1980; Sion et al. 1984; Wesemael et al. 1985) and constituted two of the four PG 1159 stars that were first analysed with non-LTE model atmospheres (Werner et al. 1991). Based on optical spectra, identical values for the basic atmospheric parameters (T_{eff} and surface gravity g) were derived for both objects: $T_{\text{eff}} =$

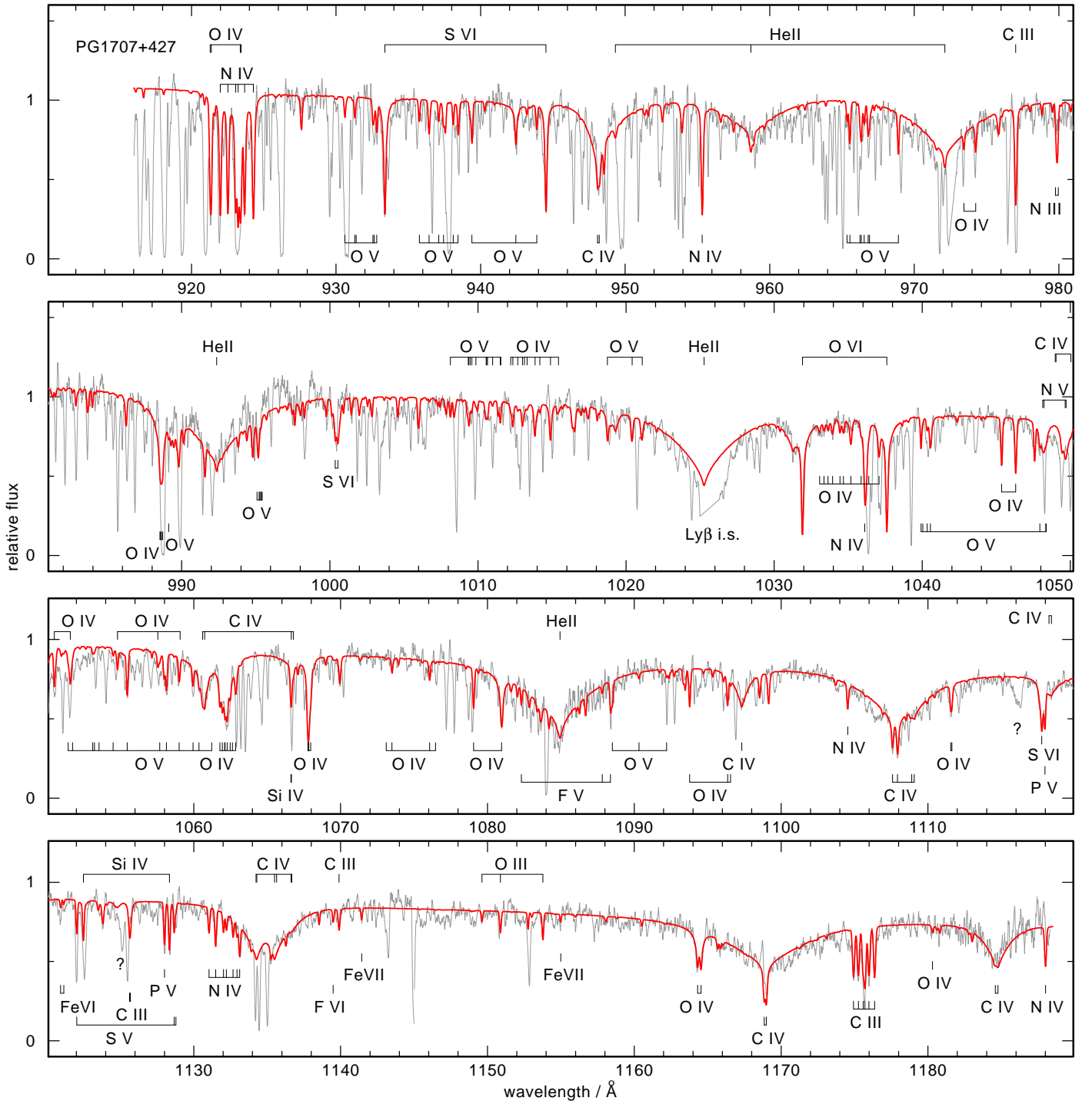


Fig. 1. FUSE spectrum of PG 1707+427 (thin line) compared to a photospheric model spectrum (thick line) with the finally adopted parameters as listed in Table 1. The main photospheric spectral lines are identified. Complete line lists are given in Tables 2–5. Question marks denote unidentified lines.

100 000 K, $\log g = 7$ (g in cm s^{-2}). Only a coarse estimate on the O abundance was possible, based on the O V 1371 Å line in poor signal-to-noise ratio (S/N) low-resolution International Ultraviolet Explorer (IUE) spectra. He/C/O abundances (given in mass fractions throughout the paper) of 0.33/0.50/0.17 were derived. Medium-resolution UV spectroscopy performed with the Goddard High Resolution Spectrograph (GHRS) aboard the Hubble Space Telescope (HST) enabled Dreizler & Heber (1998) to refine these parameters. In particular, they found that PG 1707+427 must be significantly cooler than PG 1424+535.

For PG 1707+427 $T_{\text{eff}}/\log g = 85\,000/7.5$ was derived and 110 000/7.0 for PG 1424+535.

As to the nitrogen abundance, a dichotomy was found by Dreizler & Heber (1998). From their UV spectral analysis of nine PG 1159 stars they found that four typically have $N = 0.035$, while the others have at least two or three orders of magnitude less nitrogen. PG 1707+427 and PG 1424+535 were found to belong to the former and latter groups, respectively. The abundance determination of other trace elements was only possible

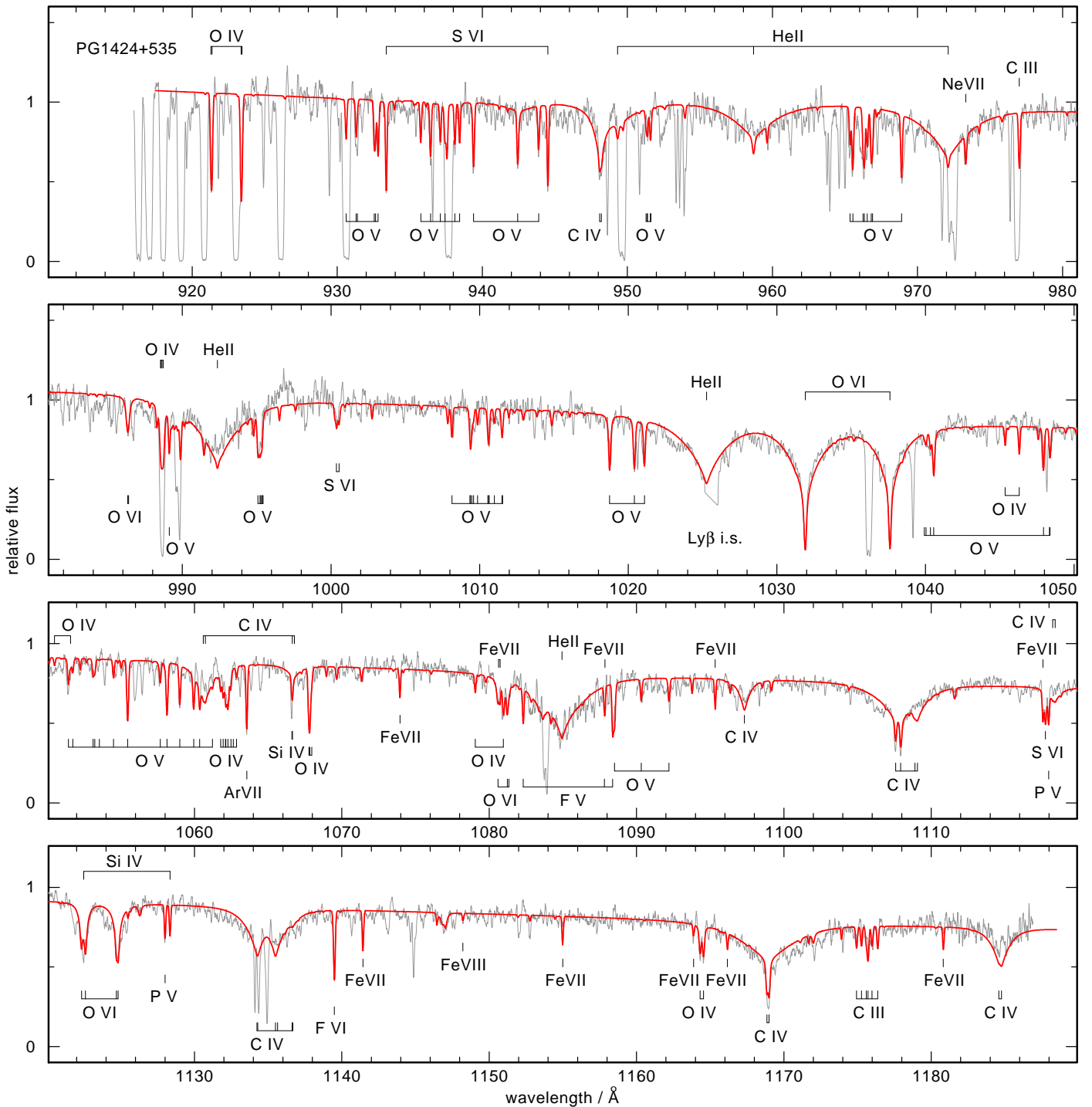


Fig. 2. As in Fig. 1, for PG 1424+535.

with the advent of FUSE. Spectral lines of F, Ne, Si, P, S, Ar, and Fe were identified, as we discuss in detail below (Sect. 5).

PG 1707+427 and PG 1424+535 are the only PG 1159 stars with $T_{\text{eff}} \lesssim 110\,000$ K that were observed with FUSE. Two other objects of this spectral class with $T_{\text{eff}} = 110\,000$ K, the central stars of the planetary nebulae Abell 43 and NGC 7094, were also observed, however, their surface gravity is much lower (hence their luminosity much higher) so that the ionization balances of all metals are shifted significantly to higher ionization stages and their line spectra are qualitatively different, including the occurrence of P Cygni line profiles (Friederich et al. 2010).

3. Observations and line identifications

The raw FUSE data for the program stars were retrieved from the Mikulski Archive for Space Telescopes (MAST). The observation IDs were P1320301 for PG 1424+535 and P1320401 for PG 1707+427. Both were observed through the LWRS spectrograph aperture, and the data were obtained in time-tag mode.

The SiC1 channel was slightly misaligned for the observation of PG 1424+535, as the SiC1 fluxes varied $\approx 15\%$ from exposure to exposure, and the net flux was $\approx 30\%$ below that measured in the other channels. The spectrum in this channel was renormalized to match that of the LiF1 spectrum at wave-

Table 1. Program stars and finally adopted parameters.^a

	PG 1707+427	PG 1424+535	Sun ^b
$T_{\text{eff}} / \text{K}$	85 000	110 000	
$\log g$	7.5	7.0	
He	0.52	0.52	0.25
C	0.45	0.45	2.4×10^{-3}
N	0.01	$\leq 3.5 \times 10^{-5}$	6.9×10^{-4}
O	0.03	0.03	5.7×10^{-3}
F	1.0×10^{-4}	5.0×10^{-5}	5.0×10^{-7}
Ne	–	1.0×10^{-2}	1.3×10^{-3}
Na	–	–	2.9×10^{-5}
Mg	$\leq 5.0 \times 10^{-3}$	$\leq 5.0 \times 10^{-3}$	7.1×10^{-4}
Al	$\leq 5.0 \times 10^{-3}$	$\leq 5.0 \times 10^{-4}$	5.6×10^{-5}
Si	3.2×10^{-4}	2.0×10^{-4}	6.6×10^{-4}
P	1.0×10^{-5}	3.2×10^{-5}	5.8×10^{-6}
S	3.2×10^{-4}	1.0×10^{-4}	3.1×10^{-4}
Ar	–	6.0×10^{-5}	7.3×10^{-5}
Ca	–	–	6.4×10^{-5}
Sc	–	–	4.6×10^{-8}
Ti	$\leq 3.1 \times 10^{-3}$	–	3.1×10^{-6}
V	$\leq 3.2 \times 10^{-5}$	$\leq 3.2 \times 10^{-4}$	3.2×10^{-7}
Cr	$\leq 1.7 \times 10^{-5}$	$\leq 1.7 \times 10^{-4}$	1.7×10^{-5}
Mn	$\leq 1.1 \times 10^{-4}$	$\leq 1.1 \times 10^{-4}$	1.1×10^{-5}
Fe	$\leq 1.3 \times 10^{-3}$	1.3×10^{-3}	1.3×10^{-3}
Co	$\leq 4.2 \times 10^{-4}$	$\leq 4.2 \times 10^{-4}$	4.2×10^{-6}
Ni	$\leq 7.1 \times 10^{-5}$	$\leq 2.0 \times 10^{-4}$	7.1×10^{-5}
Zn	$\leq 5.0 \times 10^{-6}$	$\leq 5.0 \times 10^{-6}$	1.7×10^{-6}
Ga	$\leq 5.6 \times 10^{-5}$	$\leq 1.0 \times 10^{-5}$	5.6×10^{-8}
Ge	$\leq 2.4 \times 10^{-5}$	$\leq 1.0 \times 10^{-5}$	2.4×10^{-7}
Kr	$\leq 4.0 \times 10^{-4}$	$\leq 2.0 \times 10^{-5}$	1.1×10^{-7}
Xe	$\leq 1.0 \times 10^{-5}$	$\leq 2.0 \times 10^{-6}$	1.7×10^{-8}
Ba	$\leq 1.5 \times 10^{-3}$	$\leq 1.5 \times 10^{-3}$	1.5×10^{-8}

Notes. ^(a) Abundances in mass fractions and surface gravity g in cm s^{-2} . If no abundance value is given, then no meaningful upper limit could be determined. ^(b) Solar abundances from Asplund et al. (2009).

lengths where the spectral coverage overlapped. In all other cases, the fluxes measured in any given channel were consistent to 1% or better from exposure to exposure, indicating good alignment, and consistent to within a few percent when comparing one channel to another. The net exposure times were 10.4 ksec for PG 1424+535 and 14.3 ksec for PG 1707+427.

Raw data were processed twice with CalFUSE v3.2.3: once with screening parameters set to extract data only during orbital Night, and once to extract data during orbital Day. Zero-point offsets in the wavelength scale were adjusted for each exposure by shifting each spectrum to coalign narrow interstellar absorption features. The individual exposures from each observation were then combined to form composite Day and Night spectra for each channel. The Day and Night spectra were then compared at the locations of all the known airglow emission lines. If the Day spectra showed any excess flux in comparison to the Night spectra at those wavelengths, the corresponding pixels in the Day spectra were flagged as bad and were not included in subsequent processing. Significant airglow was present during orbital Night only at Lyman β and at Lyman γ ; faint emission can be discerned at Lyman δ . This residual emission would affect fits to the interstellar absorption at these wavelengths, but has no impact on any of the analyses we present.

The final step was to combine the spectra from the four instrument channels into a single composite spectrum. Because of residual distortions in the wavelength scale in each channel, additional shifts of localized regions of each spectrum were re-

Table 2. Carbon lines identified in the FUSE spectra of at least one of our program stars.^a

Wavelength	Ion	Transition
977.02	C III	$2s^2 \ ^1S - 2s2p \ ^1P^o$
1001.99:	C III	$3p \ ^1P^o - 6d \ ^1D$
1016.34, 1016.40, 1016.53	C III	$3p \ ^3P^o - 6d \ ^3D^o$
1125.63–1125.68	C III	$3d \ ^3D^o - 6f \ ^3F^o$
1139.90	C III	$3p \ ^1P^o - 5d \ ^1D$
1165.62–1165.88 ^b	C III	$3p \ ^3P^o - 5d \ ^3D$
1174.93, 1175.26, 1175.59, 1175.71, 1175.99, 1176.37	C III	$2s2p \ ^3P^o - 2p^2 \ ^3P$
948.09, 948.21	C IV	$3s - 4p$
1048.98 ^d , 1049.02 ^d	C IV	$4d - 11f$
1050.04 ^d	C IV	$4f - 11g$
1060.59, 1060.74	C IV	$4p - 10d$
1066.63, 1066.78 ^c	C IV	$4p - 10s$
1097.32, 1097.34	C IV	$4s - 8p$
1107.59, 1107.93	C IV	$3p - 4d$
1108.89:, 1109.06:	C IV	$4p - 9d$
1118.25:, 1118.41:	C IV	$4p - 9s$
1134.25, 1134.30	C IV	$4d - 9f$
1135.50	C IV	$4f - 9g$
1135.64	C IV	$4f - 9d$
1136.63, 1136.68	C IV	$4d - 9p$
1168.85, 1168.99	C IV	$3d - 4f$
1184.59, 1184.77	C IV	$4p - 8d$

Notes. ^(a) Wavelengths in Å. Colons denote uncertain identifications of very weak or blended lines ^(b); blend Fe VI ^(c) and blend Si IV ^(d) are not included in model spectra.

Table 3. Nitrogen lines identified in PG 1707+427.

Wavelength	Ion	Transition
979.77, 979.83, 979.90, 979.97	N III	$2s2p^2 \ ^2D - 2p^3 \ ^2D^o$
989.79: ^a , 991.51: ^b , 991.58: ^b	N III	$2s^22p \ ^2P^o - 2s2p^2 \ ^2D$
1005.99:, 1006.04:	N III	$2s2p^2 \ ^2S - 2p^3 \ ^2P^o$
1183.03:	N III	$2s2p^2 \ ^2P_{1/2} - 2p^3 \ ^2P^o_{1/2}$
921.99, 922.52, 923.06, 923.22, 923.68, 924.28	N IV	$2s2p \ ^3P^o - 2p^2 \ ^3P$
948.15, 948.24, 948.29, 948.54, 948.56, 948.61 ^c	N IV	$3p \ ^3P^o - 4d^2 \ ^3D$
955.33	N IV	$2s2p \ ^1P^o - 2p^2 \ ^1S$
1036.12–1036.33	N IV	$3d \ ^3D - 4f \ ^3F^o$
1078.71	N IV	$3d \ ^1D - 4f \ ^1F^o$
1104.54	N IV	$3p \ ^1P^o - 4s \ ^1S$
1117.93	N IV	$2s3d \ ^1D - 2p3d \ ^1P^o$
1123.81	N IV	$3p \ ^1D - 4d \ ^1D^o$
1131.04, 1131.49, 1132.02, 1132.22, 1132.68, 1132.94	N IV	$2s3p \ ^3P^o - 2p3p \ ^3P$
1133.12, 1135.25, 1136.27	N IV	$2s3s \ ^3S - 2p3s \ ^3P^o$
1188.00:	N IV	$2s3s \ ^1S - 2p3s \ ^1P^o$
1018.97, 1019.29, 1019.31	N V	$4p - 6d$
1048.13, 1048.23	N V	$4d - 6f$
1049.65, 1049.71	N V	$4f - 6g$

Notes. ^(a) Dominated by N III i.s. ^(b); dominated by H₂ i.s. ^(c); blend with C IV.

quired to coalign the spectra; these shifts were typically only 1–2 pixels. Bad pixels resulting from detector defects were flagged at this point and excluded from further processing. Finally, the spectra were resampled onto a common wavelength scale and combined, weighting by S/N on a pixel-by-pixel basis.

Table 4. Oxygen lines identified in at least one of our program stars.

Wavelength	Ion	Transition
1149.63, 1150.88, 1153.77	O III	$2s2p^3\ ^3S^o - 2p^4\ ^3P$
921.30, 921.37, 923.37, 923.44	O IV	$2s2p^2\ ^2P - 2p^3\ ^2P^o$
938.47	O IV	$3p^2\ ^3P_{3/2} - 4s^2\ ^3P_{3/2}^o$
973.43: ^a , 974.25	O IV	$2s^23p^2\ ^2P^o - 2s2p3p^2\ ^2S$
994.80, 995.16, 995.17	O IV	$3p^4\ ^4D_* - 4s^4\ ^4P^o$
1013.01, 1013.86, 1014.90	O IV	$3d^4\ ^4F^o - 4f^4\ ^4F_*$
1035.18, 1037.09	O IV	$3d^4\ ^4D^o - 4f^4\ ^4D_*$
1045.36, 1046.31	O IV	$2s^23p^2\ ^2P^o - 2s^24s^2\ ^2S$
1047.59, 1050.50	O IV	$2s^23s^2\ ^2S - 2s2p3s^2\ ^2P^o$
1051.59	O IV	$3d^2\ ^4D_{5/2}^o - 4f^2\ ^4D_{5/2}$
1054.80, 1057.55, 1059.07	O IV	$3p^4\ ^4S - 4s^4\ ^4P^o$
1061.78, 1061.95, 1062.10, 1062.13, 1062.27, 1062.48, 1062.86	O IV	$3d^4\ ^4D^o - 4f^4\ ^4F$
1067.77, 1067.83, 1067.96	O IV	$3d^2\ ^2D - 4f^2\ ^2F^o$
1079.06, 1081.02, 1082.04:	O IV	$2s^23p^2\ ^2P^o - 2s2p3p^2\ ^2D$
1080.97	O IV	$3d^2\ ^4D^o - 4f^2\ ^4F_*$
1093.77, 1096.36, 1096.56:	O IV	$2s^23d^2\ ^2D - 2s2p3d^2\ ^2F^o$
1099.15:	O IV	$3p^2\ ^4D_{5/2} - 4s^2\ ^4P_{3/2}^o$
1111.56, 1111.63	O IV	$3p^4\ ^4P_* - 4s^4\ ^4P^o$
1164.32, 1164.55	O IV	$3d^2\ ^4F_* - 4f^2\ ^4G_*$
1180.31	O IV	$2s^24p^2\ ^2P_{3/2}^o - 2s2p4p^2\ ^2D_{5/2}$
931.30, 931.39, 932.64, 932.82	O V	$2s3d^3\ ^3D_* - 2p3d^3\ ^3P^o$
935.76, 936.43, 937.11, 938.11, 938.43	O V	$2s3p^3\ ^3P^o - 2p3p^3\ ^3P_*$
939.40, 942.44, 943.88	O V	$2s3s^3\ ^3S - 2p3s^3\ ^3P^o$
951.28, 951.38, 951.59, 951.62	O V	$4p^3\ ^3P^o - 6d^3\ ^3D$
959.64	O V	$4p^1\ ^1P^o - 6d^1\ ^1D$
965.35, 965.54, 966.25, 966.34, 966.53, 966.81, 966.90	O V	$2s3d^3\ ^3D - 2p3d^3\ ^3D^o$
968.90	O V	$2s3s^1\ ^1S - 2p3s^1\ ^1P^o$
988.29:	O V	$2s4d^1\ ^1D - 2p4d^1\ ^1P^o$
989.12	O V	$2s3p^3\ ^3P_1^o - 2p3p^3\ ^3S_1$
991.46	O V	$2s4d^1\ ^1D - 2p4d^1\ ^1F^o$
995.09, 995.23, 995.34	O V	$4d^3\ ^3D_* - 6f^3\ ^3F^o$
996.53:	O V	$2s3d^1\ ^1D - 2p3d^1\ ^1F^o$
1007.86, 1008.14, 1009.49, 1009.59, 1009.87, 1010.99	O V	$2s4p^3\ ^3P^o - 2p4p^3\ ^3P$
1018.78, 1020.45, 1021.13	O V	$2s4f^3\ ^3F^o - 2p4f^3\ ^3G$
1040.30	O V	$4d^3\ ^3P_3 - 6p^3\ ^3S^o$
1040.33	O V	$2s4p^3\ ^3P_2^o - 2p4p^3\ ^3S_1$
1040.56	O V	$2s4f^1\ ^1F^o - 2p4f^1\ ^1G$
1047.94	O V	$2p3d^1\ ^1F^o - 2s5g^1\ ^1G$
1048.38, 1051.45, 1051.75, 1053.13, 1053.24	O V	$2s4p^3\ ^3P^o - 2p4p^3\ ^3D_*$
1055.47, 1058.14, 1059.01, 1059.95, 1060.36	O V	$2s3p^3\ ^3P^o - 2p3p^3\ ^3D_*$
1071.34	O V	$4d^1\ ^1D - 6p^1\ ^1P^o$
1088.51 ^b	O V	$2s3p^1\ ^1P^o - 2p3p^1\ ^1P$
1090.32	O V	$2s4p^1\ ^1P^o - 2p4p^1\ ^1P$
1092.20	O V	$2s4d^1\ ^1D - 2p4d^1\ ^1D^o$
986.32	O VI	$4s - 5p$
1031.91, 1037.61	O VI	$2s - 2p$
1080.60, 1081.24, 1081.34	O VI	$4p - 5d$
1122.34, 1122.60	O VI	$4d - 5f$
1124.70, 1124.82	O VI	$4f - 5g$
1126.17, 1126.28	O VI	$4f - 5d$
1146.75, 1146.83, 1147.03	O VI	$4d - 5p$
1171.12, 1172.00	O VI	$4p - 5s$

Notes. ^(a) blend with Ne VII ^(b); blend with F V.

The final spectrum has S/N = 11–23 per 0.013Å pixel for PG 1424+535, and 9–15 per pixel for PG 1707+427. The effects of fixed-pattern noise are minimized by the fact that the positions of the spectra on the detectors varied during each observation,

Table 5. Lines of F, Ne, Si, P, S, Ar, Fe, and Ni identified in at least one of our program stars.

Wavelength	Ion	Transition
1082.31, 1087.82, 1088.39 ⁱ	F V	$2s2p^2\ ^2P - 2p^3\ ^2D^o$
1139.50	F VI	$2s2p^1\ ^1P^o - 2p^2\ ^1D$
973.33 ^h	Ne VII	$2s2p^1\ ^1P^o - 2p^2\ ^1D$
1066.61–1066.65 ^k	Si IV	$3d^2\ ^2D - 4f^2\ ^2F^o$
1122.49 ^l , 1128.34	Si IV	$3p^2\ ^2P^o - 3d^2\ ^2D$
1118.81:	Si V	$3s^3\ ^3P_2^o - 3p^3\ ^3P_2$
1000.38: ^a	P V	$3d^2\ ^2D_{3/2} - 4p^2\ ^2P_{1/2}^o$
1117.98 ^g , 1128.01 ^m	P V	$3s^2\ ^2S - 3p^2\ ^2P^o$
1039.92 ^b	S V	$3s3d^1\ ^1D - 3p3d^1\ ^1F^o$
1122.03: ^d , 1128.67, 1128.78, 1133.90:	S V	$3s3d^3\ ^3D - 3p3d^3\ ^3F^o$
933.38, 944.52	S VI	$3s - 3p$
1000.37, 1000.54	S VI	$4d - 5f$
1117.76	S VI	$4f - 5g$
1063.55 ⁿ	Ar VII	$3s3p^1\ ^1P^o - 3p^2\ ^1D$
1005.96: ^p	Fe V	$4p^5\ ^5F_{11}^o - 4d^5\ ^5G_{13}$
1115.10:	Fe VI	$4s^2\ ^4D_{5/2} - 4p^2\ ^4D_{5/2}^o$
1120.93:, 1121.15:	Fe VI	$4s^2\ ^4F - 4p^2\ ^4F^o$
1152.77: ^e	Fe VI	$4s^2\ ^4G_{7/2} - 4p^2\ ^4F_{5/2}^o$
1160.51:, 1165.67: ^f	Fe VI	$4s^2\ ^4P - 4p^2\ ^4P^o$
1073.95	Fe VII	$4s^1\ ^4D - 4p^1\ ^4P^o$
1080.64 ^o , 1080.74 ^o , 1087.86, 1095.34	Fe VII	$4s^3\ ^3D - 4p^3\ ^3P^o$
1117.58	Fe VII	$4s^1\ ^4D - 4p^1\ ^4F^o$
1141.43, 1154.99, 1166.17:	Fe VII	$4s^3\ ^3D - 4p^3\ ^3F^o$
1163.88, 1180.83:	Fe VII	$4s^3\ ^3D - 4p^3\ ^3D^o$
1062.44: ^c	Fe VIII	$4s^2\ ^4S_{1/2} - 4p^2\ ^4P_{3/2}^o$
1148.22:	Fe VIII	$4s^2\ ^4S_{1/2} - 3d^2\ ^4P_{3/2}^o$
1075.80:	Ni VI	$4s^2\ ^4I_{11/2} - 4p^2\ ^4H_{9/2}^o$
1124.19:	Ni VI	$4s^2\ ^4H_{13/2} - 4p^2\ ^4I_{15/2}^o$
1144.03:	Ni VI	$4s^2\ ^4H_{9/2} - 4p^2\ ^4I_{11/2}^o$
1154.60:	Ni VI	$4s^6\ ^6D_{7/2} - 4p^6\ ^6F_{9/2}^o$

Notes. ^(a) blend S VI ^(b); blend O V ^(c); blend O IV ^(d); blend Fe II i.s. ^(e); blend C II i.s. ^(f); blend C III ^(g); blend N IV ^(h); blend O IV ⁽ⁱ⁾; blend O V ^(k); blend Ar I i.s. and C IV ^(l); blend C I i.s. ^(m); blend Fe II i.s. ⁽ⁿ⁾; blend H₂ i.s. in PG 1707+427 ^(o); blend O IV and O VI ^(p); and blend N III.

and by the fact that nearly every wavelength bin was sampled by at least two different detectors.

The first aim of our study is to identify, as far as possible, the photospheric spectral lines in the FUSE spectra of PG 1707+427 and PG 1424+535 (Figs. 1 and 2). A similar study was performed by Jahn et al. (2007) for the prototype of the PG 1159 class, PG 1159–035, which is significantly hotter ($T_{\text{eff}} = 140\,000$ K). They found that carbon and oxygen are exclusively detected by C IV and O VI lines. In contrast, as we shall see, the spectra of our cooler program stars are dominated by lower ionization stages, namely, C III and O III-v.

Our procedure for line identification is strongly based on our synthetic model atmosphere spectra. Since the basic atmospheric parameters (T_{eff} and $\log g$) are well known, the main task in the analysis of C and O is to employ large model atoms, i.e., many energy levels and radiative transitions to predict the line spectra as completely as possible. In addition, for PG 1707+427, the N spectrum can be studied in detail. This leads to a surprisingly large number of identified lines, in comparison to the hot PG 1159 stars, and most of them were never seen in hot stars. The other metals show many fewer lines be-

Table 6. Number of levels and lines of model ions used for line formation calculations of metals.^a

	II	III	IV	V	VI	VII
C	1,0	133,745	54,279			
N		34,129	76,405	54,297		
O		47,171	83,637	105,671	9,15	
F			1,0	15,31	15,27	2,1
Ne				14,18	14,30	15,27
Na			49,39	52,229	65,301	29,80
Mg		1,0	31,93	52,175	26,55	46,147
Al		1,0	15,20	30,87	43,126	43,160
Si		17,28	30,102	25,59		
P		3,0	21,9	18,12		
S			17,32	39,107	25,48	
Ar				4,0	48,225	40,130
Kr			38,0	25,0	46,887	14,37
Xe			44,0	29,0	82,887	36,124

Notes. ^(a) First and second number of each table entry denote the number of levels and lines, respectively. The the highest ionization stage, which only comprises its ground state, is not listed for each element. For the treatment of iron-group and trans-iron elements (except of Kr and Xe), see text.

cause they are just trace elements. Only their strongest lines are detectable, which usually are transitions between relatively low excited levels so that smaller model atoms suffice. In Tables 2–4, we present all photospheric lines of C, N, and O, which we identified in at least one of our two program stars. Table 5 summarizes the lines from other metals; some of them were detected in earlier work. They are assessed in detail below (Sect. 5).

In the spectra of both stars, some likely photospheric lines remain unidentified. Two rather prominent examples in PG 1707+427 are located at 1116.2 and 1125.0 Å. They might stem from N IV multiplets with unknown wavelength position. These kinds of multiplets are predicted by our models, which include (computed) OP energy level data but do not appear in any list of observed line positions. We treat them like Kurucz’s LIN lines, namely, we do not include them in our final synthetic spectra.

To identify lines from the interstellar medium (ISM) and to judge their potential contamination of photospheric lines, we used the program OWENS (Hébrard et al. 2002; Hébrard & Moos 2003) which considers different clouds with individual radial and turbulent velocities, temperatures, column densities, and chemical compositions. Note that we did not aim to make good fits to the ISM lines. For PG 1707+427, our model includes lines of D I, H I, H₂, C I–III, N I–III, O I, P II, S II–III, Ar I, and Fe II. For PG 1424+535, our model includes lines of D I, H I, H₂ (J=0,1), C I–III, N I–III, O I, Si II, P II, Ar I, and Fe II in two clouds with radial velocities of –8 km/s and –66 km/s. This line of sight is unusual in that H₂ was just barely detectable. Figures A.1 and A.2 in the Appendix are identical to Figs. 1 and 2, but include the ISM lines.

4. Model atoms and model atmospheres

For the spectral analysis, we used our non-LTE code to compute plane-parallel, line-blanketed atmosphere models in radiative and hydrostatic equilibrium (Werner & Dreizler 1999; Werner et al. 2003). They include the three most abundant elements, namely He, C, and O. All other species were treated one by one as trace elements, i.e., keeping fixed the atmospheric structure. In the same manner, extended model atoms

for C and O were introduced, meaning that non-LTE population numbers were computed for highly-excited levels, which were treated in LTE during the preceding model-atmosphere computations. Table 6 summarizes the number of considered non-LTE levels and radiative transitions between them. All model atoms were built from the publicly available Tübingen Model Atom Database (TMAD¹), comprising data from different sources, namely Bashkin & Stoner (1975), the databases of the National Institute of Standards and Technology (NIST²), the Opacity Project³ (OP, Seaton et al. 1994), CHIANTI⁴ (Dere et al. 1997; Landi et al. 2013), as well as the Kentucky Atomic Line List⁵.

For calcium and the iron-group elements (Sc–Ni), we used a statistical approach employing typically seven superlevels per ion linked by superlines, together with an opacity sampling method (Anderson 1989; Rauch & Deetjen 2003). Ionization stages IV–VIII augmented by a single, ground-level stage IX were considered per species. We used the complete line list of Kurucz (so-called LIN lists, comprising about 3.3×10^7 lines of the considered ions; Kurucz 1991, 2009, 2011) for the computation of the non-LTE population numbers, and the so-called POS lists (that include only the subset of lines with precisely known, experimentally observed line positions) for the final spectrum synthesis.

For four trans-Fe elements (Zn, Ga, Ge, and Ba), we used the same statistical approach. The atomic data and model atoms are taken from our recent work on these species and are referred to below.

5. Results

During our spectral-line fitting procedure, we found no indication that the effective temperatures of both program stars (Dreizler & Heber 1998) require revision. That follows, for instance, from the ionization balance of oxygen. We can evaluate lines from three ionization stages in PG 1424+535 and even four in PG 1707+427. We estimate that the temperatures are known to within ± 5000 K. As to the surface gravity, the He II lines fit well with the gravity values derived by Dreizler & Heber (1998). The uncertainty in $\log g$ is 0.5 dex. In the following, we describe the derivation of element abundances in detail. For all comparisons of model spectra to the FUSE observations in the shown figures, the observations are smoothed with a 0.05 Å boxcar and the model spectra are convolved with a 0.1 Å (FWHM) Gaussian.

5.1. Abundances of He, C, N, O

The far-UV spectra of PG 1159 stars are characterized by broad lines that stem from He II and C IV (and occasionally N V). Their profiles are shaped by linear Stark effect. In the two stars considered here, the He II $n = 2 \rightarrow n'$ line series is visible from $n' = 5$ at 1085 Å, up to $n' = 10$ at 949 Å, with rapidly decreasing strength. The strongest C III lines at 977 Å and 1175–1176 Å are visible in both stars. As PG 1707+427 is cooler, it also displays a number of more, weaker C III lines. Table 2 lists all identified carbon lines.

¹ <http://astro.uni-tuebingen.de/~TMAD>

² <http://www.nist.gov/pml/data/asd.cfm>

³ <http://cdsweb.u-strasbg.fr/topbase/topbase.html>

⁴ <http://www.chiantidatabase.org>

⁵ <http://www.pa.uky.edu/~peter/atomic>

As already mentioned, the first analysis of our two program stars was based on medium-resolution optical spectra that only exhibited lines from He II and C IV. Only rough estimates for the O abundance from the O V 1371 Å line in low-resolution IUE spectra could be made. For both stars, He = 0.33, C = 0.50, O = 0.17 was claimed (Werner et al. 1991). Based on HST/GHRS UV spectra (1165–1465 Å) taken with grating G140L (resolution 0.56 Å), which allowed for the detection of C III-IV and O IV-V lines, Dreizler & Heber (1998) slightly reduced the C abundance for PG 1707+427 (He = 0.44, C = 0.39, O = 0.17) and the C and O abundances for PG 1424+535 (He = 0.50, C = 0.44, O = 0.06). From our investigation of the FUSE spectra, the reduced C/He ratio in both stars is confirmed, however, we verify the statement by Dreizler & Heber (1998) that it can only be constrained within a factor of two.

Because of the relatively high N abundance in PG 1707+427, only this star exhibits N lines. The presence of the N IV multiplet at 1131–1133 Å was first noted by Reiff et al. (2007). We identify an even larger number of N IV lines. The strongest N V lines in the model are located at 1048–1050 Å (4d–4f and 4f–6g transitions). It is blended by a similarly broad but shallower C IV feature of $n = 4 \rightarrow 11$ lines that are not included in the model. Two N III lines are detected. One near 979.9 Å is an unresolved multiplet and the other one, at 991.5 Å, are two unresolved lines of a resonance triplet. The latter, however, is probably dominated by interstellar H₂. Table 3 lists all identified nitrogen lines.

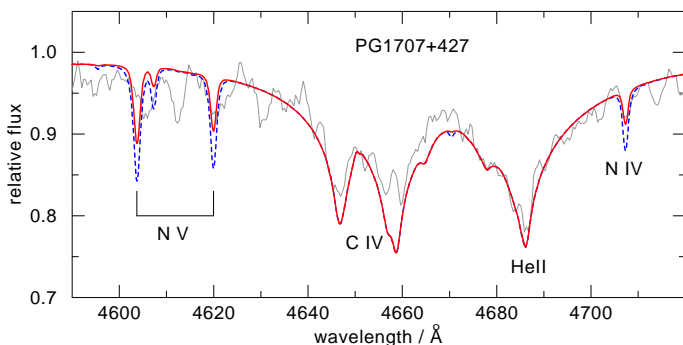


Fig. 3. Section of the optical spectrum of PG 1707+427 (thin line) centered at the He II/C IV absorption trough region. Overplotted are two models with different nitrogen abundance ($N = 0.01$ and 0.035 ; thick solid and dashed lines, respectively). Other model parameters as listed in Tab. 1.

For their nitrogen abundance analysis, Dreizler & Heber (1998) mainly relied on the N V resonance doublet. They derived $N = 0.035$ for PG 1707+427 and an upper limit of $N < 3.5 \times 10^{-5}$ for PG 1424+535. While we cannot improve the limit for PG 1424+535, the N abundance in PG 1707+427 requires a significant downward revision to $N = 0.01$, according to our FUSE data analysis. The high value derived by Dreizler & Heber (1998) must be regarded as an upper limit because an interstellar contribution to the N V resonance doublet cannot be excluded. We compared our new models with their GHRS data and find that the observed N V profile lies between the two models with $N = 0.035$ and 0.0035 , so that our low abundance from the FUSE spectra is in reasonable agreement with the GHRS data. Another constraint for the N abundance is the 3s–3p doublet, located in the optical band at 4604/4620 Å. Dreizler & Heber (1998) considered their high N abundance as compatible with the observation, however, their spectrum, taken with the TWIN spectrograph at the Calar Alto 3.5m telescope, had poor S/N. We have reobserved the star with the same equipment

but higher dispersion (36 Å/mm instead of 72 Å/mm) in 2001 and display in Fig. 3 a detail of the spectrum around the region of the absorption trough formed by He II and C IV. Overplotted are two model spectra with different N abundance. It can be seen that the high abundance model overpredicts the strength of the N V 4602/4620 Å doublet and, in addition, that of a N IV line at 4707 Å. The lower abundance fits better. The observation is smoothed with a 0.8 Å boxcar and the models with a 1 Å Gaussian. We have also inspected three optical spectra of PG 1707+427 observed by the Sloan Digital Sky Survey, however, they are of inferior quality.

As mentioned above, the far-UV spectra of the hot PG 1159 stars show many O VI lines (see Table 1 in Jahn et al. 2007), which are as strong and broad as the C IV lines because of linear Stark broadening. No oxygen lines of lower ionization stages are detectable in them. In the case of our cool PG 1159 stars, the situation is significantly different. Only a small subset of O VI lines is visible, in particular, the resonance doublet in both of our stars plus a few subordinate lines in PG 1424+535. In contrast, many lines from O IV and O V are present. In fact, the majority of all identified far-UV lines in the cool PG 1159 stars originates from these two ionization stages. In PG 1707+427, we even identify a triplet of O III. Table 4 lists all identified oxygen lines.

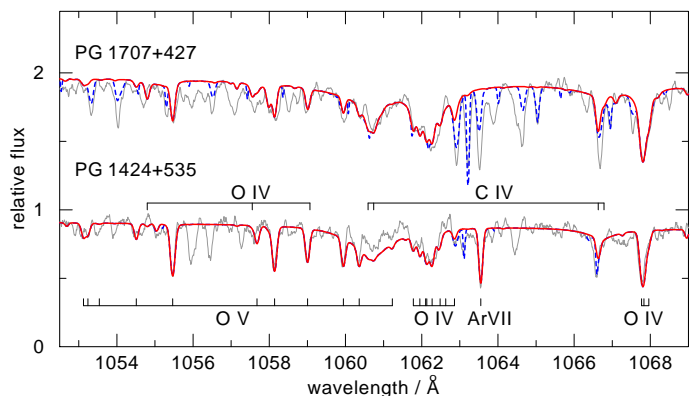


Fig. 4. Detail of the FUSE spectra shown in Figs. 1 and 2 indicating many O IV and O V lines. Interstellar lines in the models are plotted as dashed.

The oxygen abundance also needs a downward revision, namely to $O = 0.03$ for both stars, which is significantly lower in particular for PG 1707+427, so that the absolute abundances for He and C are scaled up accordingly. In Fig. 4 we show a particular wavelength region in the FUSE spectra, where a number of prominent lines of O IV and O V are located. The temperature difference between both stars is reflected by the relative line strengths of both ionization stages. Also, note the good fit to the O VI resonance doublet (second panels from top in Figs. 1 and 2), and the O III triplet in PG 1707+427 (bottom panel of Fig. 1).

The low O abundance does not contradict the HST/GHRS data, which were employed by Dreizler & Heber (1998). In Fig. 5 we show a detail of that observation compared to two models that have the high abundance claimed by Dreizler & Heber (1998) and the low abundance suggested by our FUSE data analysis. It can be seen that the strengths of the O IV lines, as well as the O V 1371 Å line, are significantly overpredicted by the more O-rich model. The GHRS observation has a resolution of 0.65 Å and was smoothed with a 0.3 Å Gaussian. Accordingly, the model spectra were smoothed with 0.72 Å Gaussians.

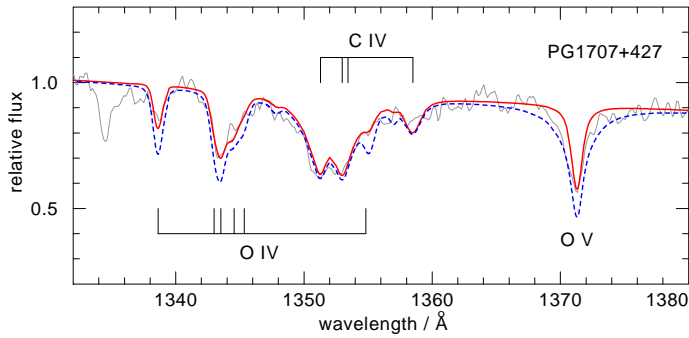


Fig. 5. Section of the HST/GHRS spectrum of PG 1707+427 (thin line). Overplotted are two models with different oxygen abundance (0.03 and 0.17; thick solid and dashed lines, respectively). Other model parameters as listed in Tab. 1.

5.2. Abundances of other metals

Abundances of F, Ne, and Ar for both stars, and Fe in PG 1424+535 were determined in previous work, but is reconsidered here with our new models. Abundances of Si, P, and S, as well as upper limits for Ni, reported in our previous progress reports, are also reassessed. Special care was taken to account for possible line blends of the CNO elements. For the first time, we also checked for the presence of Na, Mg, Al, and Ca, as well as the other iron-group elements (Sc, Ti, V, Cr, Mn, Co) and selected trans-Fe group elements (Zn, Ga, Ge, Kr, Xe, Ba). The typical error in the derived abundances is 0.3 dex unless otherwise noted.

5.2.1. Light metals (F–Ca)

Fluorine. Three F v lines (1082.3, 1087.8, 1088.4 Å) were detected in both program stars, and F vi 1139.5 Å in PG 1424+535. $F = 10^{-4}$ was derived for both objects (Werner et al. 2005). In PG 1424+535, the F vi line at 1139 Å is best suited for a model fit. In addition, we can use the two strongest components of the F v triplet at 1082 Å and 1088 Å. Care must be taken for the latter because it is blended with an O v line of similar strength. In the present work, we find $F = 5 \times 10^{-5}$ for PG 1424+535. The situation is more problematic for PG 1707+427 because of the lower S/N of the spectrum and because F vi 1139 Å is not visible because of the lower temperature. The F v 1088 Å line indicates $F = 1.0 \times 10^{-4}$. Both results essentially confirm our earlier analysis.

Neon. Ne vii λ 973.33 Å was discovered in PG 1424+535 and Ne = 0.02 was estimated (Werner et al. 2004). The line is not seen in PG 1707+427 because of its lower T_{eff} so that we cannot assess the neon abundance in this star. The weak feature in the model near this position is O iv 973.43 Å (Fig. 1). It is also visible in the model for PG 1424+535, hence, it blends the observed Ne vii line. This was unknown in our previous analyses. For PG 1424+535, we derive Ne = 1.0×10^{-2} .

Sodium. We have performed detailed line formation calculations for Na iv–vii. For both stars, there are no detectable lines in the FUSE range of our spectral models even when the abundance is as large as 10^{-2} . No meaningful upper limits can be deduced.

Magnesium. In the models for both stars, two Mg iv lines at 1044.36 and 1055.75 Å of a $^2P-^2P^o$ multiplet can be used to give an upper abundance limit (a third component with even larger gf value is blended by the O vi resonance line). We find $Mg \leq 5 \times 10^{-3}$.

Aluminium. In the model for PG 1424+535, the two strongest lines are from Al iv, namely, the 1125.61 Å component of a $^3S-^3P^o$ multiplet and a $^1P^o-^1S$ singlet at 1118.83 Å. They are used to set an upper limit of $Al < 5 \times 10^{-4}$. Weaker lines from Al v are also exhibited by the model, namely, the 1067.88 Å component of a $^4P^o-^4D$ multiplet and the 1122.87 Å component of a $^2D^o-^2F$ multiplet. In the model spectrum of the cooler star, the Al iv lines are weaker and the Al v lines have disappeared completely. We find $Al < 5 \times 10^{-3}$.

For the following discussion, we show the spectral region 1117–1133 Å in detail in Fig. 6 to demonstrate a variety of the discussed metal lines and the problem that some of them are blended with interstellar lines. Most prominent in PG 1424+535 are the broad O vi lines, which are essentially absent in PG 1707+427 because of its lower temperature.

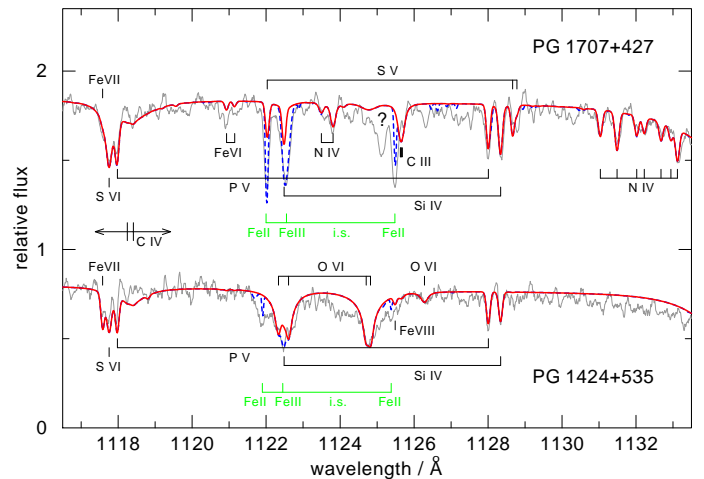


Fig. 6. Detail of the spectra shown in Figs. 1 and 2 in a region with lines from Si, P, and S. Interstellar lines in the models are plotted as dashed.

Silicon. Reiff et al. (2005) first identified Si in a PG 1159 star by the Si iv 1122.49/1128.34 Å doublet in PG 1424+535. From that, Reiff et al. (2007) estimated $Si = 3.6 \times 10^{-4}$. For PG 1707+427, they found $Si = 7.2 \times 10^{-4}$. The presence of Si v lines, discovered by Jahn et al. (2007) in the (hotter) prototype PG 1159 star, is uncertain in PG 1424+535. The Si iv doublet and Si iv 1066.63 Å are strong diagnostic lines, however, the blue component of the doublet is dominated by interstellar Fe iii 1122.52 Å, and Si iv 1066.63 Å is blended with a photospheric C iv line at the same wavelength and interstellar Ar i 1066.66 Å. Hence, relying on the 1128.34 Å line alone, we find $Si = 3.2 \times 10^{-4}$ for PG 1707+427 and 2.0×10^{-4} for PG 1424+535, which are about half the values found previously.

Phosphorus. The detection of P in a PG 1159 star was first reported by Reiff et al. (2005), who found the P v 1118/1128 Å resonance doublet in PG 1424+535. Reiff et al. (2007) estimated $P = 9.5 \times 10^{-6}$ and 2.0×10^{-6} for PG 1424+535 and PG 1707+427,

respectively. No other P lines are detectable. For the abundance analysis, care must be taken in the case of PG 1707+427 because the 1117.98 Å component of P v is coinciding with a N iv line at 1117.93 Å that is slightly weaker. We find $P = 1.0 \times 10^{-5}$. This is a compromise because at that abundance the 1118 Å component in the model is slightly too strong, while the 1128 Å component is too weak compared to the observation. Since PG 1424+535 has no detectable nitrogen, the P v 1118 Å component can safely be used for the abundance determination. Note that the line is located in the blue wing of a C iv line, and right between two lines of S vi and Fe vii. We find $P = 3.2 \times 10^{-5}$.

Sulphur. The presence of the S vi 933/945 Å resonance doublet in both stars was first noted by Reiff et al. (2005). They also reported the possible identification of S vi 1117.76 Å in PG 1424+535. From the resonance doublet, Reiff et al. (2007) derived $S = 5.0 \times 10^{-5}$ and 2.5×10^{-5} for PG 1424+535 and PG 1707+427, respectively. Another S vi doublet at 1000.5 Å is detectable in both stars, and a few S v lines are seen in PG 1707+427 (Table 5). For PG 1707+427, the best fit is achieved at $S = 3.2 \times 10^{-4}$. The S v line at 1122 Å is dominated by an interstellar Fe ii line. In PG 1424+535, no S v line is seen because of its higher temperature. From the S vi lines, we find $S = 1.0 \times 10^{-4}$. For both stars, the derived abundances are significantly higher than the previous estimates.

Argon. The hitherto only detection of Ar in a PG 1159 star is the Ar vii 1063 Å line in PG 1424+535 (Werner et al. 2007). $Ar = 3.2 \times 10^{-5}$ was derived, however, our reanalysis yields about twice that value, namely, $Ar = 6.0 \times 10^{-5}$, which is close to the solar value. The line is not accessible in PG 1707+427 because it is blended by interstellar H₂.

Calcium. There are no Kurucz POS Ca v–vii lines in the FUSE range. Lines from other Ca ions are not detectable in the models. No abundance constraints for calcium can be found.

5.2.2. Iron-group elements (Sc–Ni)

The derivation of the iron abundance and at least upper limits for the other iron group elements is of interest because they allow us to constrain the effects of radiative levitation. For example, extremely large overabundances were observed in hot subdwarfs due to this process (Heber 2009).

For scandium, only lines from ionization stage Sc v are available in the used line lists. They have relatively weak oscillator strengths. No meaningful upper abundance limits can be derived because even at 10^4 times solar Sc abundance no significant line is detected in the model spectra. For titanium, only lines from Ti v are in the line lists for the FUSE range. They are very weak in the models for PG 1707+427 and even weaker in the models for PG 1424+535. An upper limit can be derived only for the former, from the Ti v line blend at 1153.26 and 1153.28 Å. A few very weak vanadium lines appear in the models. From the three strongest, V v 1142.74, 1157.57, and 1159.52 Å, we derive upper abundance limits. In the models for PG 1707+427, the strongest chromium lines are Cr v 1104.30 Å and Cr vi 957.01 Å. For PG 1424+535, the Cr v line disappears and the Cr vi line becomes weaker. Only weak manganese lines, Mn v (1055.98 Å) and Mn vi 927.61, 933.78, 1113.58 Å, are noticeable in the models.

Fe vii lines were detected in PG 1424+535 and a solar abundance was derived (Werner et al. 2011). Two Fe viii lines are possibly present in PG 1424+535 (Table 5); they were first discovered in hotter PG 1159 stars by Werner et al. (2011). Because of the lower temperature, the Fe vii lines are not clearly detectable in PG 1707+427. Weak lines from Fe vi could be expected but their identification is uncertain as well (Table 5). According to our models, the strongest line of Fe v is at 1005.96 Å, but it is blended with N iii. We confirm the solar abundance in PG 1424+535 found previously. Since iron lines cannot be detected beyond doubt, we can only derive an upper limit for PG 1707+427.

Only rather weak cobalt lines of Co vi (e.g., 1128.75 and 1172.88 Å) are present in the models. Our models with solar Ni abundance predict only weak nickel lines. The four strongest are from Ni vi (Table 5). In the model for PG 1707+427, their strengths are just below the detection limit regarding the S/N of the observation. An upper abundance limit of solar can be derived, confirming Reiff et al. (2008). Because of the higher T_{eff} , the Ni vi lines in the model for PG 1424+535 are even weaker. No nickel line of higher ionization stages is available in the Kurucz POS lists.

5.2.3. Trans-iron group elements: Zn, Ga, Ge, Kr, Xe, and Ba

These elements have been detected in the FUSE spectrum of the hot DO white dwarf RE 0503–289 ($T_{\text{eff}} = 70\,000$ K, $\log g = 7.5$) with extreme overabundances. The star is considered a PG 1159–DO transition object and it is therefore interesting to check whether these elements are overabundant in PG 1159 stars as well. In particular, six species were studied in detail, namely, Kr and Xe (Werner et al. 2012), Zn (Rauch et al. 2014a), Ga (Rauch et al. 2015), Ge (Rauch et al. 2012), and Ba (Rauch et al. 2014b). In those papers, the strongest lines of these elements were identified in the models and the observation. None of these species is detected in our stars and we derived the upper abundance limits listed in Tab. 1 after the following considerations.

The models for both stars exhibit a large number of Zn v lines. The strongest are located at 1116.85, 1138.25, and 1142.93 Å, and there is a strong blend of several lines at 1177 Å. Numerous lines of Ga v and Ga vi are seen in the models for PG 1707+427, while in the models for PG 1424+535, only Ga vi lines are present. Just as many lines of Ge v and Ge vi in the models behave like the respective gallium lines. The strongest features are Ge v 1045.71 and 1072.66 Å as well as Ge vi 926.82 Å. The strongest krypton line in the models is Kr vii 918.14 Å, and the strongest xenon lines are Xe vii 995.51 and 1077.12 Å. In the models for PG 1707+427, the strongest lines of barium are from Ba vi (937.24 and 953.39 Å) and Ba vii (943.10 and 993.41 Å). In the models for PG 1424+535, the Ba vi lines are no longer visible.

6. Summary and discussion

We have analyzed the far-UV spectra of two relatively cool PG 1159 stars to derive elemental abundances and to compare them with predictions from stellar-evolution theory. The only other PG 1159 star hitherto investigated in similar detail is the prototype itself (PG 1159–035, Jahn et al. 2007). The resulting abundance values are listed in Table 1 and displayed in Fig. 7. The analysis was performed with non-LTE model atmosphere calculations employing vastly extended and new model atoms as compared to our earlier, exploratory assessments of these stars.

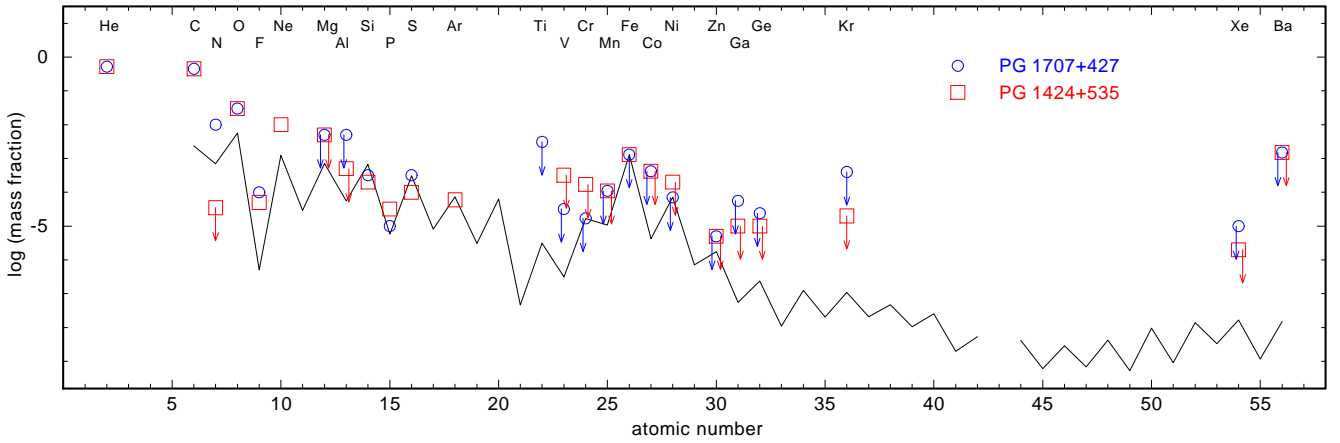


Fig. 7. Derived elemental abundances. Upper limits are marked with arrows. Solar abundance values are indicated with the black line.

Complete compilations of all identified photospheric lines are presented.

Considering the numerous ionization balances of the different species, we found no hint that effective temperatures and surface gravities determined by previous work based on optical and UV spectra require revision. Consequently, the masses derived by comparison with evolutionary tracks (Fig. 8, Werner & Herwig 2006; Althaus et al. 2009) also remain unaltered. The masses are $M = 0.53$ and $0.51 M_{\odot}$ for PG 1707+427 and PG 1424+535, respectively. Considering the initial-final mass relation by Weidemann (2000), this corresponds to about one solar mass for their main-sequence progenitors. However, the error in $\log g$ (0.5 dex) means that the masses could be as high as 0.7 and $0.58 M_{\odot}$, corresponding to 3.5 and $2.5 M_{\odot}$ progenitors.

While we confirmed the C/He ratio in the stars, the mass fraction of oxygen was found to be significantly lower compared to earlier work (Dreizler & Heber 1998). For both stars, we find $O = 0.03$ instead of 0.17 and 0.07 for PG 1707+427 and PG 1424+535, respectively. This value is relatively low compared to the prototype PG 1159–035 with $O = 0.17$, but identical to three other cool PG 1159 stars reanalyzed recently with high-resolution optical spectra (Werner & Rauch 2014). Likewise, the N abundance in PG 1707+427 was reduced from $N = 0.035$ to 0.01 , and the Ne abundance in PG 1424+535 from $Ne = 0.02$ to 0.01 . Concerning trace elements, the abundances of other light metals (F, Si, P, S, Ar) were reassessed and, in some cases, revised. The solar Fe abundance in PG 1424+535 was confirmed. Upper limits for most other iron-group elements (Ti, V, Cr, Mn, Co, Ni) as well as some trans-iron elements (Zn, Ga, Ge, Kr, Ce, Ba) were derived for the first time.

Our discussion on the element abundances is mainly based on a comparison with stellar evolution models by Shingles & Karakas (2013), who presented intershell abundances for stars with initial masses of 1.8 – $6 M_{\odot}$. They compared their results to abundances derived for the prototype PG 1159–035. In general, good agreement was found for the species investigated (He, C, O, F, Ne, Si, P, S, Fe) with the notable exception of sulphur, for which a strong depletion (0.02 times solar) in PG 1159–035 was claimed by Jahn et al. (2007), who speculated that the very slight depletion of S by n-capture nucleosynthesis predicted by stellar models (0.6 solar) could point to modeling problems of the AGB intershell chemistry. In addition, one possible solution of the so-called sulphur anomaly in planetary nebulae, which describes an unexplained S depletion (Henry et al. 2004), could originate from sulfur transformation into chlorine by neutron captures and subsequent beta decay in the central star’s preceding AGB

phase. Consequently, Shingles & Karakas (2013) have examined to what extent particular uncertainties of nucleosynthesis modeling (nuclear reaction rates, mass width of partially mixed zone) can affect the resulting intershell abundances of stars with a variety of initial masses. However, no explanation for the sulphur anomaly could be found. In contrast to the prototype, in the two stars of the present study we find $S = 1/3$ solar and solar, which is in agreement with stellar models.

While the carbon abundance in our two stars ($C = 0.45$) is in agreement with the value found for the prototype ($C = 0.48$), the oxygen abundance is significantly lower ($O = 0.03$ compared to 0.17). Nevertheless, the various C and O abundances are consistent with models that include overshoot into the C–O core (Werner & Herwig 2006). (Such high values are not exhibited in the Shingles & Karakas (2013) models because they do not include that strong overshoot.) As to nitrogen, the presence of ample N in one of our stars was already discovered by Dreizler & Heber (1998). It is explained by the fact that the late thermal pulse had occurred in this star when it was already a WD (so-called very late TP), leading to ^{14}N production by H ingestion and burning. The absence (or much smaller) N abundance in the other star is the consequence of the late thermal pulse that the progenitor suffered during its previous H-shell burning post-AGB phase.

Our study has confirmed the previously found extreme overabundance of fluorine in our two stars as well as other PG 1159 stars including the prototype, which is consistent with stellar models (see Werner et al. 2005, and discussion therein). In particular, the abundances found in PG 1707+427 and PG 1424+535 (10 and 5×10^{-5}) are consistent with the range of abundances in models with different mass and reaction rates presented by Shingles & Karakas (2013) (2 – 8×10^{-5}), although their lowest mass model ($1.8 M_{\odot}$) falls short by factors of 2.5 and 5 to correctly predict the observed high F abundances.

Generally, neon was found to be strongly enriched in PG 1159 stars to typical values of $Ne = 0.02$ (Werner et al. 2004), in agreement with stellar models (where ^{14}N is transformed into ^{22}Ne by two α captures). The neon abundance we find in PG 1424+535 is half that value but, regarding our error estimate, this is not significantly below the predictions.

Our results on the silicon abundance (0.3 – 0.5 solar) are, within error limits, consistent with the model predictions by Shingles & Karakas (2013) (0.7 – 0.9 solar). For phosphorus, we find 5.5 solar for PG 1424+535, matching the P overproduction of four times solar predicted by the $1.8 M_{\odot}$ model of Shingles

& Karakas (2013). For PG 1707+427, 1.7 solar was determined, matching the 1.9 solar overproduction of P in a 3.0 M_{\odot} model.

We have investigated the possibility of discovering other light metals that were not detected before in PG 1159 stars. It turned out that Na, Mg, Al, and Ca are undetectable even at strongly oversolar abundances (Tab. 1).

The solar iron abundance found in PG 1424+535 (and other PG 1159 stars, Werner et al. 2011) was confirmed and is in agreement with the Shingles & Karakas (2013) stellar models. They predict a slight Fe reduction of about 30%, a small amount that is not verifiable by our analysis. For all other iron-group elements except of scandium, upper abundance limits were derived. Their nondetection is consistent with solar values and excludes overabundances of more than 1–2 dex as detected in hot subdwarfs as a consequence of radiative levitation (Heber 2009).

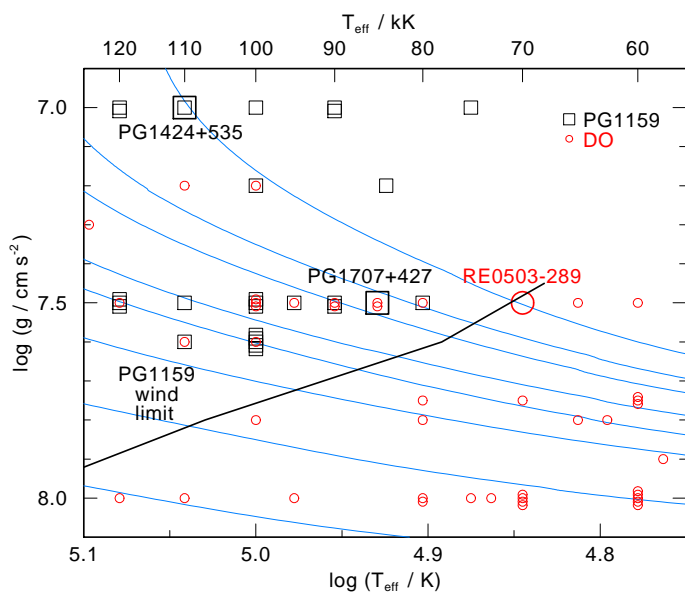


Fig. 8. Position of PG 1159 stars (squares) and DO white dwarfs (circles) in the $\log g - T_{\text{eff}}$ diagram. Our two program stars and a particular DO are indicated with big symbols and name tags. Blue lines are evolutionary tracks by Althaus et al. (2009) with stellar masses of 0.514, 0.530, 0.542, 0.565, 0.584, 0.609, 0.664, and 0.741 M_{\odot} (from top to bottom). The black line is the PG 1159 wind limit (see text).

For the first time, we assessed the question as to the presence of trans-Fe elements in PG 1159 stars. This was inspired by the recent discovery of extreme overabundances in the hot DO white dwarf RE 0503–289 ($T_{\text{eff}} = 70\,000$ K, $\log g = 7.5$, $M = 0.51 M_{\odot}$), which is believed to be an object in the PG 1159–DO transition phase (Fig. 8) evolving across the so-called wind limit (Unglaub & Bues 2000), when gravitational settling and radiative acceleration of elements begin to affect the chemical surface composition. For six elements (Zn, Ga, Ge, Kr, Xe, Ba), 155–23 000 times solar values were derived (Rauch et al. 2015, and references therein), corresponding to mass fractions in the range $0.3\text{--}3.5 \times 10^{-4}$. We have not found any trace of these species in the two investigated PG 1159 stars, but from the determined upper abundance limits (Table 1) the following can be concluded.

We do not see an enrichment of these elements as extreme as in RE 0503–289, in particular, the abundances of Zn, Ge, and Xe in RE 0503–289 are above the detection thresholds in PG 1707+427 by factors of 54, 6, and 6, and by factors of 54, 15, 31 in PG 1424+535, respectively. In the latter star, Ga and Kr, if present as abundant as in RE 0503–289, would also be above the detection threshold by factors of 2 and 3. It is proba-

ble that in RE 0503–289 these elements are driven to such very high abundances by radiative levitation.

What abundances of the trans-iron elements do we find in the intershell of AGB star models and how do they compare to our detection thresholds? In stellar AGB nucleosynthesis models of a 2 M_{\odot} star (Gallino priv. comm., Karakas et al. 2007), the following values are found after the 30th thermal pulse: Zn = 2.2×10^{-6} , Ga = 2.7×10^{-7} , Ge = 5.9×10^{-7} , Kr = 1.9×10^{-6} , Xe = 1.5×10^{-6} , and Ba = 1.2×10^{-5} . A comparison with Table 1 shows that the detection thresholds of zinc in both stars (Zn = 2.2×10^{-6}) and of xenon in PG 1424+535 (Xe = 2.0×10^{-6}) are just barely higher, while the abundances of the other elements are well below the respective limits. Spectra of better S/N would allow the detection of at least Zn, Xe, and Kr.

In summary, far-UV spectroscopy of relatively cool PG 1159 stars is essential to determine abundances of light and heavy metals beyond C, N, and O. The light metals (F–Ar) are generally in good agreement with evolution models. We do not find extreme overabundances of iron-group and trans-iron group elements, which is consistent with the expectation that radiative levitation and gravitational settling are not affecting the abundance patterns in these stars. The detection of trans-iron elements would be valuable to constrain parameters of the s-process nucleosynthesis modeling, but far-UV spectra with better S/N are required.

Finally, a particular aspect of the pulsation properties of PG 1159 stars is interesting. Nonpulsating stars exist in the respective GW Vir instability strip. The nitrogen dichotomy mentioned in Sect. 2 led Dreizler & Heber (1998) to conclude that nitrogen is an essential ingredient for pulsation driving because the nonpulsators have low N abundances. On the other hand, it was shown that it is predominantly the high O abundance that is responsible for pulsation driving (e.g., Quirion et al. 2007). We found that our two program stars have the same O (and C) abundance, while the N abundance is significantly different. Curiously, PG 1707+427 ($N = 0.01$) is a pulsator and PG 1424+535 ($N < 3.5 \times 10^{-5}$) is a nonpulsator, which would confirm the conclusion by Dreizler & Heber (1998). We recently obtained a similar result from an analysis of three other cool PG 1159 stars (Werner & Rauch 2014).

Acknowledgements. T. Rauch is supported by the German Aerospace Center (DLR) under grant 05 OR 1402. This research has made use of the SIMBAD database, operated at CDS, Strasbourg, France, and of NASA’s Astrophysics Data System Bibliographic Services. Some of the data presented in this paper were obtained from the Mikulski Archive for Space Telescopes (MAST). This work had been done using the profile fitting procedure Owens.f, developed by M. Lemoine and the FUSE French Team.

References

- Althaus, L. G., Panei, J. A., Miller Bertolami, M. M., et al. 2009, *ApJ*, 704, 1605
- Anderson, L. S. 1989, *ApJ*, 339, 558
- Asplund, M., Grevesse, N., Sauval, A. J., & Scott, P. 2009, *ARA&A*, 47, 481
- Bashkin, S. & Stoner, J. O. 1975, *Atomic energy levels and Grotrian Diagrams - Vol.1: Hydrogen I - Phosphorus XV; Vol.2: Sulfur I - Titanium XXII*
- Dere, K. P., Landi, E., Mason, H. E., Monsignori Fossi, B. C., & Young, P. R. 1997, *A&AS*, 125, 149
- Dreizler, S. & Heber, U. 1998, *A&A*, 334, 618
- Friederich, F., Rauch, T., Werner, K., Koesterke, L., & Kruk, J. W. 2010, in *American Institute of Physics Conference Series*, Vol. 1273, American Institute of Physics Conference Series, ed. K. Werner & T. Rauch, 231
- Heber, U. 2009, *ARA&A*, 47, 211
- Hébrard, G., Friedman, S. D., Kruk, J. W., et al. 2002, *Planet. Space Sci.*, 50, 1169
- Hébrard, G. & Moos, H. W. 2003, *ApJ*, 599, 297
- Henry, R. B. C., Kwitter, K. B., & Balick, B. 2004, *AJ*, 127, 2284
- Jahn, D., Rauch, T., Reiff, E., et al. 2007, *A&A*, 462, 281

- Karakas, A. I., Lugaro, M., & Gallino, R. 2007, *ApJ*, 656, L73
- Kurucz, R. L. 1991, in *NATO ASIC Proc. 341: Stellar Atmospheres - Beyond Classical Models*, ed. L. Crivellari, I. Hubeny, & D. G. Hummer, 441
- Kurucz, R. L. 2009, in *American Institute of Physics Conference Series*, Vol. 1171, American Institute of Physics Conference Series, ed. I. Hubeny, J. M. Stone, K. MacGregor, & K. Werner, 43
- Kurucz, R. L. 2011, *Canadian Journal of Physics*, 89, 417
- Landi, E., Young, P. R., Dere, K. P., Del Zanna, G., & Mason, H. E. 2013, *ApJ*, 763, 86
- Liebert, J. & Stockman, H. S. 1980, *PASP*, 92, 657
- Müller-Ringat, E. M. 2013, Dissertation, Eberhard Karls Universität Tübingen
- Quirion, P.-O., Fontaine, G., & Brassard, P. 2007, *ApJS*, 171, 219
- Rauch, T. & Deetjen, J. L. 2003, in *Astronomical Society of the Pacific Conference Series*, Vol. 288, *Stellar Atmosphere Modeling*, ed. I. Hubeny, D. Mihalas, & K. Werner, 103
- Rauch, T., Werner, K., Biémont, É., Quinet, P., & Kruk, J. W. 2012, *A&A*, 546, A55
- Rauch, T., Werner, K., Quinet, P., & Kruk, J. W. 2014a, *A&A*, 564, A41
- Rauch, T., Werner, K., Quinet, P., & Kruk, J. W. 2014b, *A&A*, 566, A10
- Rauch, T., Werner, K., Quinet, P., & Kruk, J. W. 2015, *A&A*, 577, A6
- Reiff, E., Jahn, D., Rauch, T., et al. 2007, in *Astronomical Society of the Pacific Conference Series*, Vol. 372, *15th European Workshop on White Dwarfs*, ed. R. Napiwotzki & M. R. Burleigh, 237
- Reiff, E., Rauch, T., Werner, K., & Kruk, J. W. 2005, in *Astronomical Society of the Pacific Conference Series*, Vol. 334, *14th European Workshop on White Dwarfs*, ed. D. Koester & S. Moehler, 225
- Reiff, E., Rauch, T., Werner, K., Kruk, J. W., & Koesterke, L. 2008, in *Astronomical Society of the Pacific Conference Series*, Vol. 391, *Hydrogen-Deficient Stars*, ed. A. Werner & T. Rauch, 121
- Seaton, M. J., Yan, Y., Mihalas, D., & Pradhan, A. K. 1994, *MNRAS*, 266, 805
- Shingles, L. J. & Karakas, A. I. 2013, *MNRAS*, 431, 2861
- Sion, E. M., Liebert, J., Starrfield, S., & Wesemael, F. 1984, in *NASA Conference Publication*, Vol. 2349, *NASA Conference Publication*, ed. J. M. Mead, R. D. Chapman, & Y. Kondo, 273–276
- Unglaub, K. & Bues, I. 2000, *A&A*, 359, 1042
- Weidemann, V. 2000, *A&A*, 363, 647
- Werner, K., Deetjen, J. L., Dreizler, S., et al. 2003, in *Astronomical Society of the Pacific Conference Series*, Vol. 288, *Stellar Atmosphere Modeling*, ed. I. Hubeny, D. Mihalas, & K. Werner, 31
- Werner, K. & Dreizler, S. 1999, *Journal of Computational and Applied Mathematics*, 109, 65
- Werner, K., Heber, U., & Hunger, K. 1991, *A&A*, 244, 437
- Werner, K. & Herwig, F. 2006, *PASP*, 118, 183
- Werner, K. & Rauch, T. 2014, *A&A*, 569, A99
- Werner, K., Rauch, T., & Kruk, J. W. 2005, *A&A*, 433, 641
- Werner, K., Rauch, T., & Kruk, J. W. 2007, *A&A*, 466, 317
- Werner, K., Rauch, T., Kruk, J. W., & Kurucz, R. L. 2011, *A&A*, 531, A146
- Werner, K., Rauch, T., Reiff, E., Kruk, J. W., & Napiwotzki, R. 2004, *A&A*, 427, 685
- Werner, K., Rauch, T., Ringat, E., & Kruk, J. W. 2012, *ApJ*, 753, L7
- Wesemael, F., Green, R. F., & Liebert, J. 1985, *ApJS*, 58, 379

Appendix A: Model spectra including ISM lines

Figures A.1 and A.2 are identical to Figs. 1 and 2, except they include the ISM lines. The pure photospheric spectrum is plotted in red, while the additional ISM lines are indicated in blue.

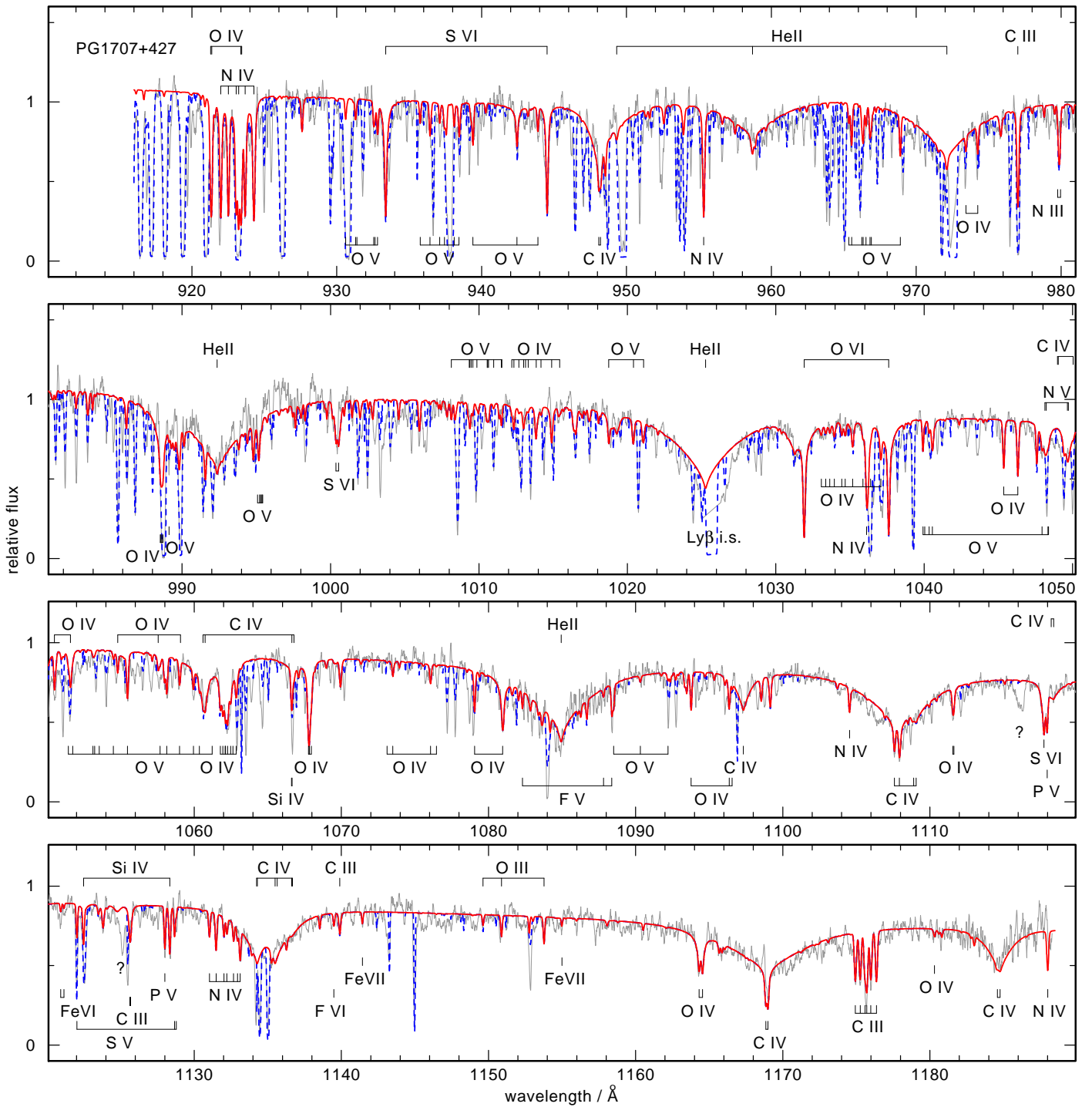


Fig. A.1. As in Fig. 1, except that it includes ISM lines (dashed graph).

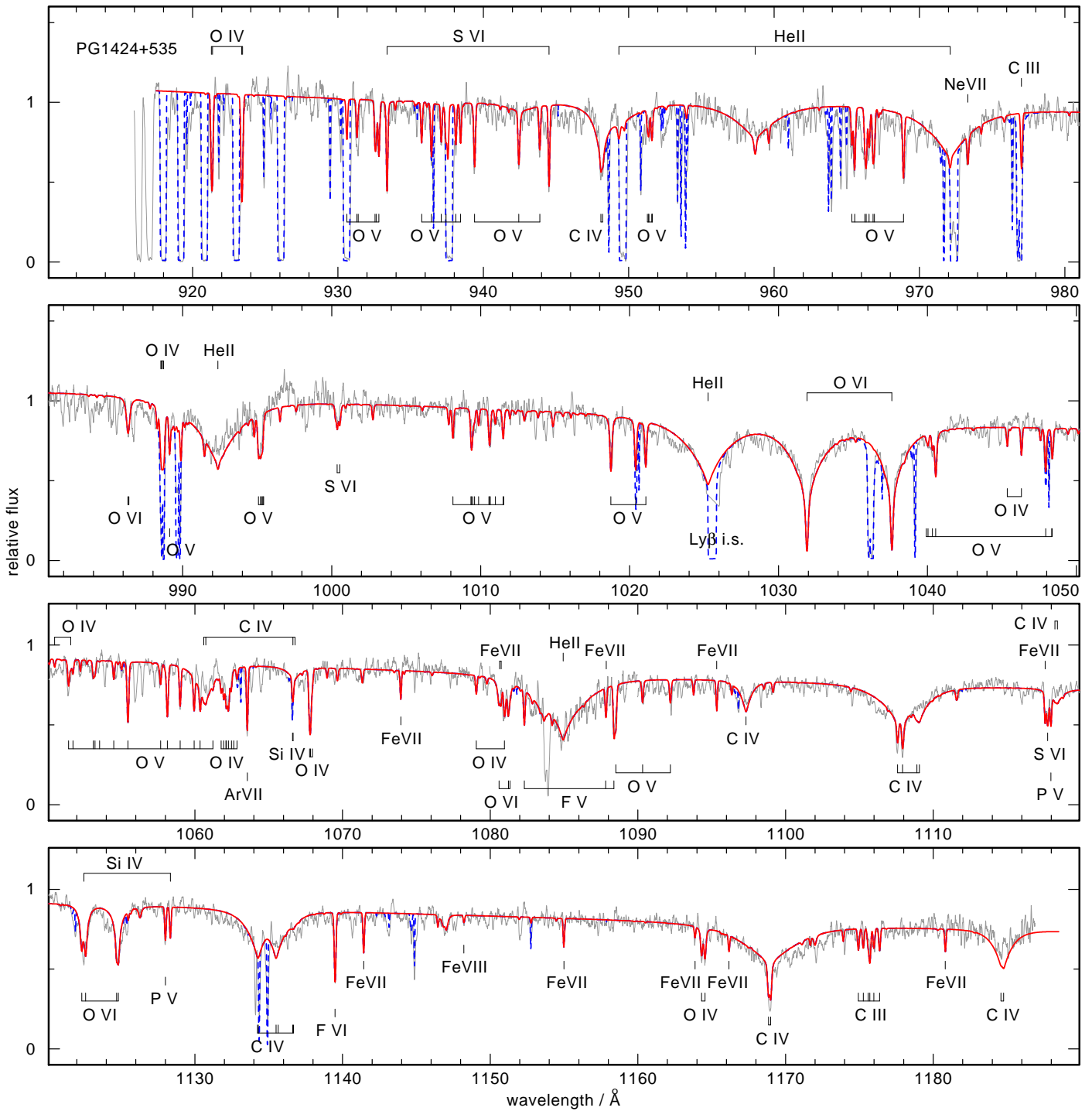


Fig. A.2. As in Fig. 2, except that it includes ISM lines (dashed graph).